UC Irvine
UC Irvine Previously Published Works

Title
Substrate-Dependent Allosteric Regulation in Cytochrome P450cam (CYP101A1)

Permalink
https://escholarship.org/uc/item/1gd7b4jw

Journal
Journal of the American Chemical Society, 140(47)

ISSN
0002-7863

Authors
Follmer, Alec H
Mahomed, Mavish
Goodin, David B
et al.

Publication Date
2018-11-28

DOI
10.1021/jacs.8b09441

Copyright Information
This work is made available under the terms of a Creative Commons Attribution License, available at https://creativecommons.org/licenses/by/4.0/

Peer reviewed

eScholarship.org Powered by the California Digital Library
University of California

JACS
JOURNAL OF THE AMERICAN CHEMICAL SOCIETY
Article
Cite This: J. Am. Chem. Soc. 2018, 140, 16222−16228
pubs.acs.org/JACS

Substrate-Dependent Allosteric Regulation in Cytochrome P450cam (CYP101A1)

Alec H. Follmer,[†] Mavish Mahomed,[‡,#] David B. Goodin,[‡] and Thomas L. Poulos*[,†]

[†]Departments of Molecular Biology and Biochemistry, Pharmaceutical Sciences, and Chemistry, University of California, Irvine, California 92697-3900, United States

[‡]Department of Chemistry, University of California, Davis, California 95616, United States

Supporting Information

ABSTRACT: Various biophysical methods have provided evidence of a second substrate binding site in the well-studied cytochrome P450cam, although the location and biological relevance of this site has remained elusive. A related question is how substrate and product binding and egress occurs. While many active site access channels have been hypothesized, only one, channel 1, has been experimentally validated. In this study, molecular dynamics simulations reveal an allosteric site related to substrate binding and product egress. The remote allosteric site opens channel 1 and primes the formation of a new channel that is roughly perpendicular to channel 1. Substrate entry to the active site via channel 1 as well as substrate/product egress via channel 2 is observed after binding of a second molecule of substrate to the allosteric site, indicating cooperativity between these two sites. These results are consistent with and bring together many early and recent experimental results to reveal a dynamic interplay between a weak allosteric site and substrate binding to the active site that controls P450cam activity.

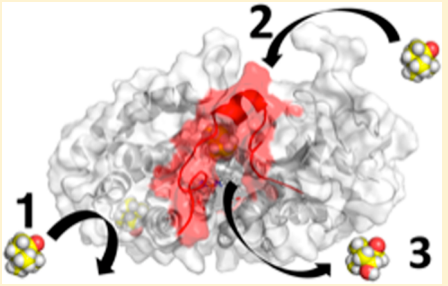

INTRODUCTION

Cytochromes P450, heme-containing mono-oxygenases found in all kingdoms of life, represent an important family of enzymes responsible for drug detoxification, and participate in the biosynthesis of steroids and a variety of natural products.[1] The most thoroughly investigated P450, P450cam (CYP101A1) from *Pseudomonas putida*, catalyzes the hydroxylation of D-camphor to 5-*exo*-hydroxycamphor, which initiates the oxidative assimilation of camphor as an energy source. Since P450cam was the first P450 to be sequenced, purified in large quantities, and have its crystal structure determined, this P450 has served as a paradigm for mechanistic and structure−function studies.[2−14] Several additional P450 crystal structures have shown that the overall P450 fold is conserved as are some critical catalytic residues. These similarities have strengthened the view that many of the conclusions based on P450cam studies are broadly applicable to other P450s.

The highly conserved fold and sequestered heme cofactor raises the question of whether substrate entry and product exit occur via the same or different channels and if those channels are conserved across P450s. The open substrate-free structure of P450cam[15] revealed that large motions of the F and G helices expose the active, thus providing a route for substrate entry (Figure 1).

The crystal structure of the P450cam−Pdx complex[17,18] shows that the binding of Pdx shifts P450cam more toward the open form that is basically the same open structure solved in the absence of Pdx.[15] The Pdx-induced shift toward the open state is also observed in solution using double electron−electron resonance methods[19,20] while isothermal titration calorimetry

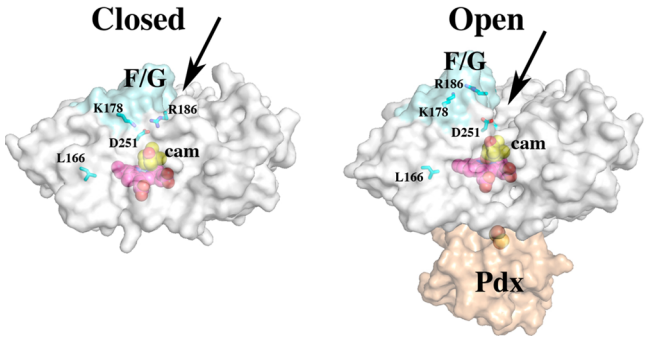

Figure 1. Structure of closed and open P450cam showing the location of the P450cam ferredoxin redox partner, Pdx. The proposed substrate access channel is indicated by the arrows. This is the region of the structure that experiences the largest open/close motion. In the closed state, Asp251 is tied up with ion pairs to Lys178 and Arg186 but in the open state Asp251 is free to serve its role in a proton relay network required for O_2 activation. Also shown is Leu166 which NMR studies[16] have shown is perturbed by camphor binding and is the allosteric binding site proposed in this study. (PDB: 2CPP and 4JWU).

shows that Pdx favors binding the open form of P450cam.[19,21] The open/close motion is dominated by movement of the F/G helices that provides a direct path to the distal side of the sequestered heme iron (Figure 1).[17,22] This motion is associated with substrate binding that displaces the iron-linked aqua ligand shifting the P450 from the six-coordinate low-spin open to the

Received: August 31, 2018
Published: October 30, 2018

ACS Publications © 2018 American Chemical Society

DOI: 10.1021/jacs.8b09441
J. Am. Chem. Soc. 2018, 140, 16222−16228

five-coordinate high-spin closed state (Figure 2). In P450cam, it generally has been assumed that substrate entry and product

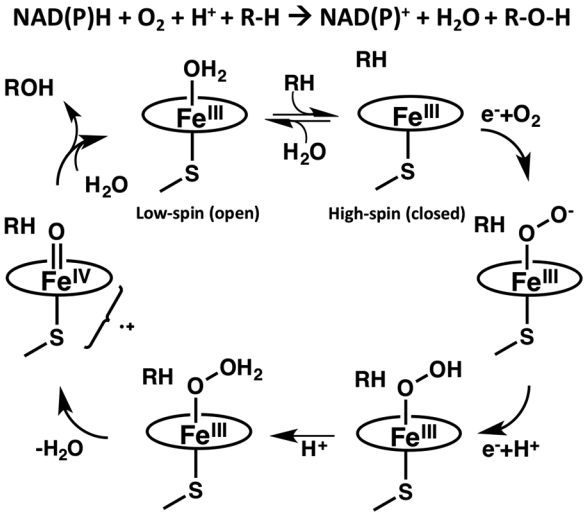

Figure 2. P450 catalytic cycle.

egress occur through the same access channel defined by the F/G helical region (Figure 1). However, different entry and exit channels would be more efficient and compatible with the requirement of maintaining high turnover. Indeed, well-crafted steered molecular dynamics simulations suggest alternate routes for substrate/product binding, although this possibility has not been experimentally verified.[23−26] Related to understanding routes to/from the active site is experimental support for a second camphor binding site quite some distance from the active site. Our molecular dynamics simulations to be presented in this paper identify a novel second camphor binding site that controls substrate entry and formation of a second active site access channel. These results provide a detailed structural basis for explaining several previously published results.

COMPUTATIONAL METHODS

Molecular dynamics (MD) simulations were performed as previously described.[27,28] In brief, one structure was used for the simulations, the P450cam open structure in 4JX1 where Pdx was removed. The P450cam in this structure is basically the same as the open P450cam crystal structure solved without Pdx (3L62).[15] The rms deviation of Cα atoms between the two structures is 0.37 Å. We chose 4JX1 because in this structure the entire protein is clearly defined in electron density maps while in 3L62 residues 91−94 and 104 are not visible. Therefore, using 4JX1 required no modeling to obtain a complete structure for MD simulations. The protein was solvated in a rectangular box of TIP3 waters with a 10 Å cushion and Na^+ ions were added to maintain net neutrality. Asp297, which is buried in the active site and forms a H-bond with a heme propionate, was protonated. Camphor was placed manually on the distal side of the protein for simulations including external camphor. One molecule was introduced near the known entry channel and the second and third at a distance ∼10 Å from the protein, near the cutoff distance for long-range interactions in our simulations. Structures were minimized for 1000 cycles, allowing only H atoms and solvent molecules to move followed by an additional 1000 cycles where all atoms were allowed to move. Production runs were then carried out using Amber 14 or Amber 16.[29] To sample functionally important time scales, we first utilized a technique known as hydrogen mass repartitioning (HMR).[30] In brief, the size of simulation time steps is dictated by the fastest vibrations that occur in the system, which are H atom vibrations. By repartitioning masses of heavy atoms to their adjacent hydrogen atoms, one can effectively slow down the vibrations of these bonds while preserving the overall mass of the system, thereby not increasing viscosity. This allows larger time steps to be taken to capture large conformational motions that take place over longer intervals, effectively cutting the computational time in half. We later found that motions relevant to allosteric interactions and camphor binding did not require the time scales necessitating HMR. For HMR runs, topology files were modified by the *parmed.py* python script and both protein and water masses were repartitioned using the command *HMassrepartition dowater*.[30] HMR runs were performed using 4 fs time steps and non-HMR runs were performed using traditional 2 fs steps suggested by the SHAKE algorithm. All simulations were performed using a random initial velocity with each run having a different initial velocity (ig = −1). Two runs were carried out using HMR and 4 fs time steps for ∼1.4 μs each with three molecules of camphor. Three runs with HMR and 4 fs time steps were performed with 1 molecule of camphor for 1.6 μs, 350 ns, and 310 ns. Five additional runs using 2 fs time steps and no repartitioning were performed for 1 μs. Five runs were performed for 500 ns with no camphor in the simulation. Data analysis was carried out in cpptraj and VMD.[31,32] Trajectory images were produced in Pymol (Schrodinger).

RESULTS AND DISCUSSION

Identification of an Allosteric Camphor Site. Our initial goal was to see if camphor placed in the solvent cushion surrounding the protein would diffuse through channel 1, between the F/G loop and B'-helix, and bind near the heme. To simulate camphor in solution binding to substrate-free P450cam, three camphor molecules were placed in the solvent cushion, giving an effective threefold excess, an experimentally relevant condition, and within the limit of solubility of camphor in water given the size of the solvent box. In all of these simulations, a molecule of camphor binds to a pocket on the "back side" of the F/G helices between the C/D/E/F helices (Figure 3). This site is defined by V118, V123, K126, L127,

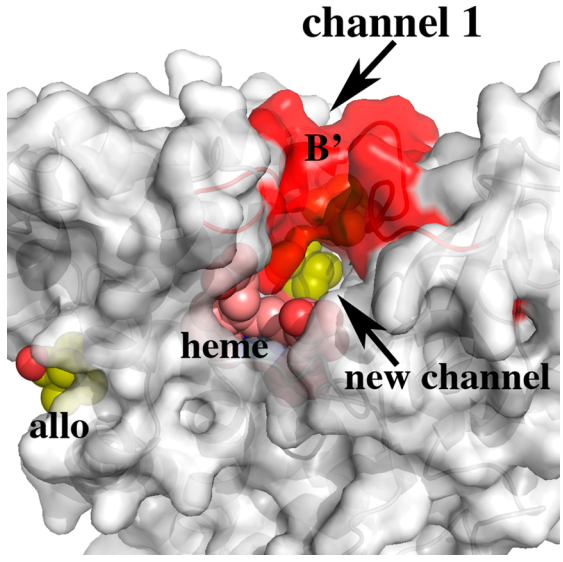

Figure 3. Location of the proposed allosteric (labeled **allo**) camphor binding site. Camphor (yellow) is tucked into a hydrophobic pocket between the C and E helices.

L166, and T217 (Figure 3). This is the same region that NMR studies found is perturbed in the presence of high camphor concentrations.[16,33]

These NMR results can be interpreted as either camphor binding to the active site resulting in long-range perturbations at the L166 site or direct binding of camphor to the L166 region.

DOI: 10.1021/jacs.8b09441
J. Am. Chem. Soc. 2018, 140, 16222−16228

Our MD simulations indicate that perturbation of L166 could be due to direct interactions between camphor and L166.

Binding to this allosteric site also is accompanied by widening of channel 1 as well as formation of a new active site access channel 2 (Figure 4). This second channel was formerly

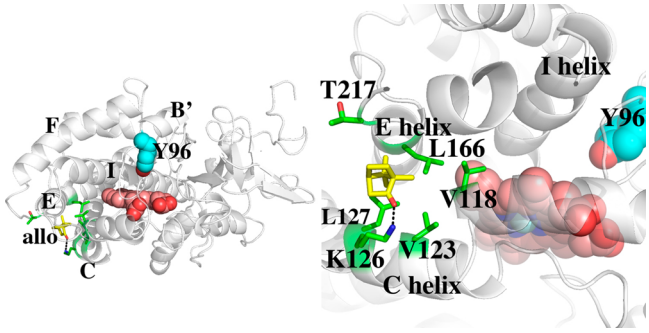

Figure 4. Structure of P450cam at 378 ns. Binding of camphor (yellow) to the allosteric site results in the opening of a new active site access channel.

identified as a possible egress channel using modified molecular dynamics techniques such as random expulsion MD (REMD) and metadyanmics.[23,25] Cojocaru et al.[23] also suggested the formation of this new channel, but neither the REMD nor metadynamics studies postulated allostery or explored the correlation of channel formation with a second camphor site. We found that a good measure of channel 2 formation is the distance between the Cα atoms of S83 and S102, which is ~5 Å in the closed structures and ~7−13 Å when channel 2 is open. Experimentally, S83 was identified by Asciutto et al.[34] as a hinge region that undergoes sizable chemical shifts in the absence of camphor. Using the S83−S102 distance as a criterion for channel 2 formation, we find a strong correlation between occupancy of the allosteric site and formation of this new channel (Figure 5). When there is no substrate present in our simulations, the S83−S102 distance fluctuates between 5 and 7 Å (Figure 5). Upon addition of a single camphor in the crystallographic pose, channel 2 remains shut at 5 Å. Binding of camphor to the allosteric site shifts the S83−S102 distance to ~7 Å. In simulations where both binding and egress events occur, the second channel opens to nearly 12 Å and the open state is strongly preferred.

If binding to the allosteric site results in formation of a more open active site and binding to that site is much weaker than to the active site, then binding ought to favor low-spin P450cam at high concentrations of camphor. Indeed, multiple studies have found that, at concentrations of camphor well beyond that required for saturating the active site, P450cam shifts back toward low spin.[35−38] This was attributed to the binding of a second camphor molecule and is consistent with our results where camphor binding to the L166 allosteric site opens the active site, thereby shifting P450cam toward low spin. At the time of these equilibrium binding studies, the location and relevance of this site was not known. Our simulations also are consistent with the NMR work of Yao et al.[39] In this study, a second camphor site with a $K_D \approx 43$ μM was located 15−16 Å from the heme iron by paramagnetic T_1 relaxation. Uniform labeling with ^{13}C Thr showed that a Thr residue is perturbed at high camphor concentrations, but peak overlap prevented determination of its exact location.[39] The allosteric site in our simulations fit these data well as it is ~15 Å from the heme iron

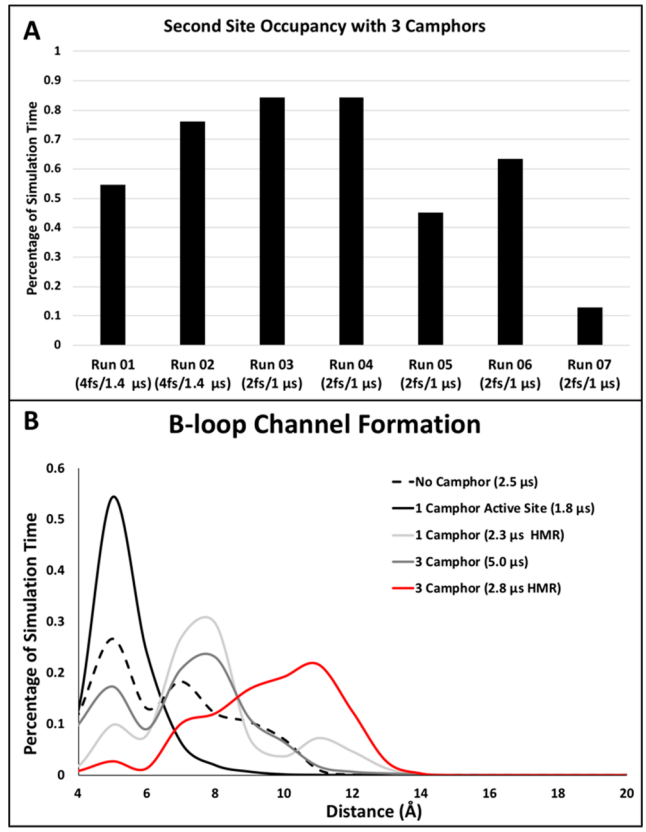

Figure 5. (A) Camphor population in the allosteric binding pocket as percentage of simulation time. Run 01 and run 02 were performed with 4 fs time steps and HMR for 1.4 μs each. Runs 03−07 were 1 μs each and utilized 2 fs time steps and no HMR. (B) B loop residues S83−S102 Cα distance as a percentage of total aggregate time in simulations containing no camphor (black dashed), one camphor in its crystallographic pose (black solid), one molecule using HMR (solid dark gray), three camphor molecules with 2 fs steps (solid light gray), and 4 fs steps and HMR (solid red).

and T217 is in the allosteric pocket. Finally, Colthart et al. found that the L166A mutant in the presence of excess camphor favors high-spin P450cam, even though enzyme activity was decreased.[16] Camphor binding to the L166 allosteric site should be weakened in the L166A mutant, and as a result, excess camphor will no longer favor low-spin P450cam. Our MD simulations and allosteric site hypothesis are consistent with NMR[16,39] and equilibrium binding data.[14,35,37]

Crystallographic Support for the Allosteric Binding Site. Direct observation of camphor binding to our proposed allosteric site would require trapping P450cam in a thermodynamic local minimum of the substrate-free open form and then introducing substrate. This is precisely what Lee et al.[15] accomplished in solving the crystal structure of substrate-free P450cam in the open state (3L62). In this structure, the B′ helix (residues 91−94) is not visible in the electron density because of disorder, which opens channel 2 in a similar way to what we observe in the MD simulations. In a separate study, Liou et al.[19] soaked these same substrate-free P450cam crystals in excess camphor and found that camphor binds in the active site but in multiple conformations (5IK1). If our allosteric model is correct, then we would expect to observe camphor binding to our proposed allosteric site in the 5IK1 structure. We therefore re-examined the electron density maps for both structures (Figure 6). In the camphor-soaked structure, there is a peak of

DOI: 10.1021/jacs.8b09441
J. Am. Chem. Soc. 2018, 140, 16222−16228

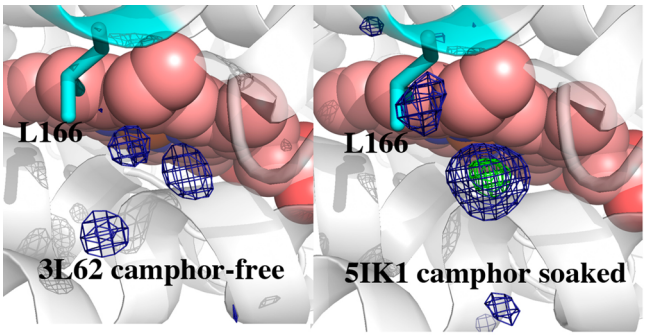

Figure 6. Fo−Fc electron density maps contoured at 4.0σ (blue) and 7.0σ (green). In the substrate-free 3L62 structure the lobes of electron density are consistent with water molecules as originally modeled. However, in the 5IK1 structure the much larger electron density is not consistent with ordered water but with a much larger molecule(s). Since the only difference in the two experiments is soaking with camphor in 5IK1, the larger lobe of electron density near L166 is consistent with an orientationally disordered camphor.

electron density at 7σ near our proposed allosteric site which is not seen in the camphor-free structure. This is consistent with a weakly bound orientationally disordered camphor bound to the allosteric site as predicted by our MD simulations.

An Allosteric Model. The rather dramatic effects of camphor binding to the allosteric site on access channel formation offers a dynamic picture relevant to catalysis and cooperativity. This also provides evidence for the growing realization of how weak transient allosteric interactions can serve to prime and direct enzymatic catalysis.[40,41] A series of snapshots derived from one of the HMR simulations is shown in Figure 7. After ~60 ns, one camphor molecule binds to the allosteric site, pulling back on the F/G lid, thus widening channel 1 so a molecule of camphor is able to enter the active site. Substrate binding to the allosteric site also pulls on the B′ to C-helix loop

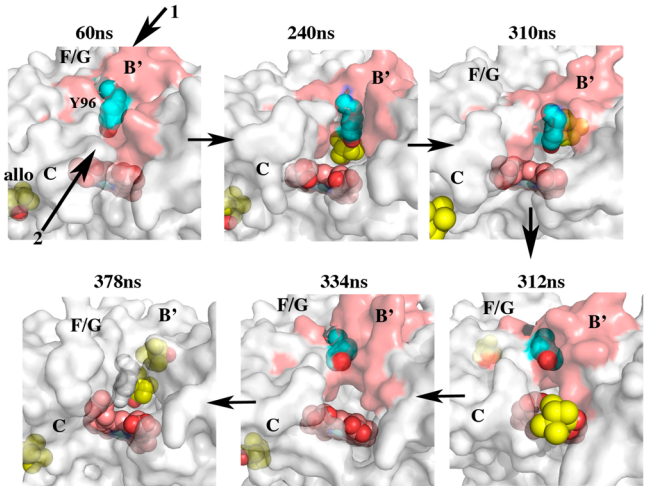

Figure 7. Two relevant channels are indicated by 1 and 2. **60 ns:** A camphor molecule (yellow) binds to the allosteric site (allo), priming channel 2 to open. **240 ns:** Binding of a second molecule to the active site widens channel 2. Between 240 and 310 ns, one molecule dissociates from the allosteric site. **310−312 ns:** The active site molecule is swept from the active site via Tyr96 (cyan) through the B′ region. **334 ns:** A new molecule binds to the allosteric site. **378 ns**: Y96 flips back to the active site upon binding two molecules substrate, restarting the cycle.

through mechanical coupling, creating a second channel to the active site (Figure 7, channel 2). This is seen in every simulation we performed. This long-range coupling from the allosteric site to the substrate access channel (about 10 Å) allows for a second molecule of camphor to enter the active site. Once the camphor enters the active site via channel 1 in the 250 ns time range, the F/G helices tighten down on the substrate, which weakens binding to the allosteric site so camphor dissociates from the allosteric site. At 312 ns, the substrate molecule is ejected through channel 2 and Y96 flips out toward solvent. That Y96 can adopt both the "in" and "out" orientations is consistent with crystal structures of P450cam in the open state.

Binding to the allosteric site favors the more open form which enables a second camphor molecule to enter the active site and the formation of channel 2 that provides a pathway for rapid substrate binding and product egress. Y96 operates as a swinging arm to "grab" entering substrates when Y96 is in the "up" orientation and then in the "in" orientation helps to hold camphor in position for stereo- and regioselective hydroxylation. Product then can depart via channels 1 or 2, but our data suggests that the channel is unidirectional: entry via channel 1; egress via channel 2. Since active site binding favors the closed form, there is a dynamic interplay between the closed/open transition and active site/allosteric site binding.

We observe additional changes that are consistent with NMR studies as detailed by Colthart et al.[16] With use of a combination of mutagenesis and chemical shifts, it was demonstrated that I160 in the E helix and L250 in the I helix are mechanically coupled. In our HMR simulations where egress is observed, the side chains of Ile160 and L250 have a correlation coefficient of 0.910 over 1.4 μs (1), where C is the average correlation, V is a motion vector per frame, and N is the total number of frames.

$$C(a, b) = \frac{\sum Va \cdot Vb}{N} \quad (1)$$

With an average distance of 7.67 ± 1.05 Å, the fluctuations in distance between the two side chains are driven by events of binding and dissociation at the allosteric and active site (Figure S1, Supporting Information). In our simulations, just as Colthart et al.[16] describe, it is this coupling that allows the I helix to undergo a deformation upon substrate binding and straightening upon camphor ejection/removal from the active site (Movie S2).

Allostery and Redox Partner Binding. The cooperative interaction between the allosteric site and active site also has relevance to the binding of Pdx. Since both Pdx binding and allosteric site binding promote the open form, then Pdx and allosteric site binding work synergistically and promote each other's binding. In addition, both Pdx binding and allosteric site binding promote the same structural changes at the Pdx docking site. L358 is positioned at the Pdx binding docking site and must adopt an alternate rotamer conformation when Pdx binds (Figure 8). As shown in Figure 8, the L358 N-Cα-Cβ-Cγ dihedral is ca. −70° in the closed (2CPP) and substrate-free open (3L62) structures.[2,15] However, in the P450cam−Pdx complexes (4JX1, 4JWU, and 3W9C) the L358 dihedral ranges between 55° and 65°.[17,18] This change is necessary to enable Pdx to form a tighter interface with P450cam. Our simulations show that when the allosteric site is occupied with camphor, the L358 rotamer becomes more flexible, and when substrate is driven through channel 2, the rotamer is the same as in the P450cam−Pdx complex where P450cam is open. Therefore, the allosteric site is coupled to not only the active site but also the Pdx docking

DOI: 10.1021/jacs.8b09441
J. Am. Chem. Soc. 2018, 140, 16222−16228

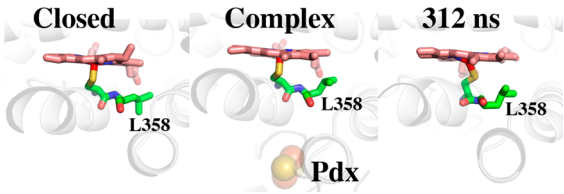

Figure 8. L358 adopts a different rotamer in the closed and open states. In the open conformer when Pdx is bound or when the allosteric site is occupied, L358 rotates up to contact the heme.

site. When L358 is in the Pdx-bound conformation, the Leu side chain is closer to the heme and thus "pushes" on the proximal face of the heme. There is good evidence that this "push" effect is coupled to changes on the opposite of the heme that favors the open form of P450cam. When O_2 binds to ferrous P450cam, the I helix undergoes a significant widening that enables catalytic waters to move into place as part of proton relay network required for O_2 activation. The direction of I helix motion is from closed to partially open. CO, often used as an O_2 mimic, causes none of these changes in wild-type P450cam but the CO-L358P mutant more closely mimics those changes induced by O_2 binding.[42] This indicates that the L358P mutant can more easily adopt the open conformation.[42−44] The structural basis for these effects is that the more rigid sterically restricted P358 side chain "pushes" on the proximal face of the heme and these changes are transmitted to distal side and I helix. Thus, the L358P mimics the close to open switch accompanying Pdx binding and camphor binding to the allosteric site. This suggests how two unique interfaces can be presented for electron transfer upon binding of Pdx with and without substrate in the allosteric site. Binding at the allosteric site which favors open P450cam also favors Pdx binding. As suggested by Tripathi et al.,[17] the closed state is inactive because the proton relay network involving the essential Asp251 is locked down by tight salt bridges. However, in the open state these salt bridges are broken, thus enabling Asp251 to serve its function in proton transfer to the iron-linked dioxygen.

We close our discussion with the potential biological implications of these results. While seemingly quite complex, the logic of these transitions in the requirements for balancing rapid turnover with association/dissociation processes and the utilization of camphor as a carbon source is rather simple. The expression of P450cam, PdR, and Pdx is under the control of the CamR repressor, although the P450cam proteins are constitutively expressed at low levels in the absence of camphor.[45] Therefore, at low camphor concentrations, the active site, but not the allosteric site, is occupied and the enzyme is in the closed inactive conformation. At higher camphor concentrations, where camphor now can be used as a carbon source, the allosteric site comes into play and together with Pdx binding switches P450cam to the more open active conformation. This view is consistent with what is known about how the CamR repressor that controls the expression of P450cam, Pdx, and Pdr. CamR is released from the CamR regulatory DNA sequence only at high camphor concentrations.[46] Like many dimeric bacterial repressors, CamR binds two ligand (in this case, camphor) molecules. The first exhibits a $K_D \approx 0.06$ μM, but CamR remains bound to the CamR regulatory DNA sequence. Binding of the second camphor molecule with a $K_D \approx 14$ μM results in the release of CamR and expression of the P450cam gene products. This means P450cam and its redox supporting proteins are highly expressed only at high levels of camphor, >10 μM, which is well above the K_D for camphor binding to the P450cam active site. Therefore, the entire CamR system including the low amounts of constitutively expressed P450cam are shutdown at low levels of camphor where camphor cannot serve as a useful carbon source, thus avoiding the unnecessary consumption of NADH.

CONCLUSIONS

The results of our MD simulations provide a detailed structural model on the allosteric interplay between substrate binding, redox partner interactions, and O_2 activation that are consistent with a wealth of experimental data. Most importantly, the novel allosteric binding site identified in this study is consistent with NMR and crystallographic data[16,19,39] as well as equilibrium binding data.[37] Changes in specific residues observed in our simulations also are consistent with mutagenesis data as well as differences observed in the crystal structures of the open and closed states. From these simulations, it is clear how allosteric regulation in P450cam favors the open conformation and can stimulate formation of a second channel for product egress, the role of Tyr96, as well as the distortion of the I helix and long-range mechanical couplings. Such strong correlation with experiments provides a high level of confidence that the allosteric site identified in our simulations and the changes associated with substrate entry and egress provides a realistic structural model of allostery in P450cam. One possible advantage for such a level of allosteric control is to ensure that neither substrate binding/product egress are limiting under steady-state conditions. Therefore, at high levels of camphor the kinetic processes of substrate binding and allostery are masked and, as observed experimentally, the first electron transfer step becomes limiting.[19]

ASSOCIATED CONTENT

Supporting Information

The Supporting Information is available free of charge on the ACS Publications website at DOI: 10.1021/jacs.8b09441.

Figure of mechanical coupling of the residues I150 and L252 to occupancies of the active and allosteric site (PDF)

Morphed snapshots of consecutive frames of a simulation undergoing camphor egress over a period of 2 ns; a molecule of camphor (yellow) held in the active site undergoes egress through the B−C loop (red); tyrosine-96 (cyan) rotates from the inward facing position to being solvent-exposed; heme is in orange and I160 and L250 are in green (MOV)

The same consecutive frames of a simulation undergoing camphor egress over a period of 2 ns as seen in the first movie; highlighting the mechanical coupling of I160 (green-left) and L250 (green-right) as camphor (yellow) is driven from the active site: Y96 (cyan) and heme (orange) (MOV)

Surface representation between three sequential MD snapshots of unbound, allosteric site bound, and active site bound; this morph demonstrates allosteric site binding priming channel 2 (red) formation and binding to the active site further opens the channel 2 prior to egress (MOV)

A molecular dynamics simulation written every 2 ns; camphor (yellow) binds to the allosteric site (0:00−0:10) near L166 (red); a second molecule then enters the active

DOI: 10.1021/jacs.8b09441
J. Am. Chem. Soc. 2018, 140, 16222−16228

site (0:11) and the allosteric site molecule dissociates (0:38); this is followed by egress and Y96 (cyan) flipping from the active site (0:43); finally, a molecule of camphor rebinds to the allosteric site (MOV)

AUTHOR INFORMATION

Corresponding Author

*poulos@uci.edu

ORCID

Alec H. Follmer: 0000-0002-6244-6804

David B. Goodin: 0000-0002-9196-0001

Thomas L. Poulos: 0000-0002-5648-3510

Present Address

#Gilead Sciences, 333 Lakeside Drive, Foster, California 94404.

Notes

The authors declare no competing financial interest.

ACKNOWLEDGMENTS

This work was supported by NIH grant GM57353 (TLP) and GM41049 (DBG). The authors would like to acknowledge the San Diego Supercomputing Center (SDSC) for the use of the Triton Shared Computing Cluster (TSCC).

REFERENCES

(1) Poulos, T. L. Heme enzyme structure and function. *Chem. Rev.* **2014**, *114*, 3919−3962.

(2) Poulos, T. L.; Finzel, B. C.; Gunsalus, I. C.; Wagner, G. C.; Kraut, J. The 2.6-A crystal structure of Pseudomonas putida cytochrome P-450. *J. Biol. Chem.* **1985**, *260*, 16122−16130.

(3) Gunsalus, I. C.; Wagner, G. C. Bacterial P-450cam methylene monooxygenase components: cytochrome m, putidaredoxin, and putidaredoxin reductase. *Methods Enzymol.* **1978**, *52*, 166−188.

(4) Katagiri, M.; Ganguli, B. N.; Gunsalus, I. C. A soluble cytochrome P-450 functional in methylene hydroxylation. *J. Biol. Chem.* **1968**, *243*, 3543−3546.

(5) Dus, K.; Katagiri, M.; Yu, C. A.; Erbes, D. L.; Gunsalus, I. C. Chemical characterization of cytochrome P-450cam. *Biochem. Biophys. Res. Commun.* **1970**, *40*, 1423−1430.

(6) Yu, C.; Gunsalus, I. C. Crystalline cytochrome P-450cam. *Biochem. Biophys. Res. Commun.* **1970**, *40*, 1431−1436.

(7) Tsai, R.; Yu, C. A.; Gunsalus, I. C.; Peisach, J.; Blumberg, W.; Orme-Johnson, W. H.; Beinert, H. Spin-state changes in cytochrome P-450cam on binding of specific substrates. *Proc. Natl. Acad. Sci. U. S. A.* **1970**, *66*, 1157−1163.

(8) Haniu, M.; Armes, L. G.; Tanaka, M.; Yasunobu, K. T.; Shastry, B. S.; Wagner, G. C.; Gunsalus, I. C. The primary structure of the monoxygenase cytochrome P450CAM. *Biochem. Biophys. Res. Commun.* **1982**, *105*, 889−894.

(9) Sligar, S. G.; Gunsalus, I. C. A thermodynamic model of regulation: modulation of redox equilibria in camphor monoxygenase. *Proc. Natl. Acad. Sci. U. S. A.* **1976**, *73*, 1078−1082.

(10) Lipscomb, J. D.; Sligar, S. G.; Namtvedt, M. J.; Gunsalus, I. C. Autooxidation and hydroxylation reactions of oxygenated cytochrome P-450cam. *J. Biol. Chem.* **1976**, *251*, 1116−1124.

(11) Gunsalus, I. C.; Sligar, S. G. Redox regulation of cytochrome P450cam mixed function oxidation by putidaredoxin and camphor ligation. *Biochimie* **1976**, *58*, 143−147.

(12) Gunsalus, I. C.; Sligar, S. G. Equilibrium states and dynamic reactions of iron in the camphor monoxygenase system. *Adv. Exp. Med. Biol.* **1976**, *74*, 254−262.

(13) Lange, R.; Hui Bon Hoa, G.; Debey, P.; Gunsalus, I. C. A thermodynamic-kinetic analysis of the cytochrome P-450 heme pocket. *Acta. Biol. Med. Ger.* **1979**, *38*, 143−152.

(14) Hui Bon Hoa, G.; Di Primo, C.; Dondaine, I.; Sligar, S. G.; Gunsalus, I. C.; Douzou, P. Conformational changes of cytochromes P-450cam and P-450lin induced by high pressure. *Biochemistry* **1989**, *28*, 651−656.

(15) Lee, Y. T.; Wilson, R. F.; Rupniewski, I.; Goodin, D. B. P450cam visits an open conformation in the absence of substrate. *Biochemistry* **2010**, *49*, 3412−3419.

(16) Colthart, A. M.; Tietz, D. R.; Ni, Y.; Friedman, J. L.; Dang, M.; Pochapsky, T. C. Detection of substrate-dependent conformational changes in the P450 fold by nuclear magnetic resonance. *Sci. Rep.* **2016**, *6*, 22035.

(17) Tripathi, S.; Li, H.; Poulos, T. L. Structural basis for effector control and redox partner recognition in cytochrome P450. *Science* **2013**, *340*, 1227−1230.

(18) Hiruma, Y.; Hass, M. A.; Kikui, Y.; Liu, W. M.; Olmez, B.; Skinner, S. P.; Blok, A.; Kloosterman, A.; Koteishi, H.; Lohr, F.; Schwalbe, H.; Nojiri, M.; Ubbink, M. The structure of the cytochrome p450cam-putidaredoxin complex determined by paramagnetic NMR spectroscopy and crystallography. *J. Mol. Biol.* **2013**, *425*, 4353−4365.

(19) Kuznetsov, V. Y.; Poulos, T. L.; Sevrioukova, I. F. Putidaredoxin-to-cytochrome P450cam electron transfer: differences between the two reductive steps required for catalysis. *Biochemistry* **2006**, *45*, 11934−11944.

(20) Myers, W. K.; Lee, Y. T.; Britt, R. D.; Goodin, D. B. The conformation of P450cam in complex with putidaredoxin is dependent on oxidation state. *J. Am. Chem. Soc.* **2013**, *135*, 11732−11735.

(21) Hollingsworth, S. A.; Batabyal, D.; Nguyen, B. D.; Poulos, T. L. Conformational selectivity in cytochrome P450 redox partner interactions. *Proc. Natl. Acad. Sci. U. S. A.* **2016**, *113*, 8723−8728.

(22) Poulos, T. L.; Finzel, B. C.; Howard, A. J. High-resolution crystal structure of cytochrome P450cam. *J. Mol. Biol.* **1987**, *195*, 687−700.

(23) Cojocaru, V.; Winn, P. J.; Wade, R. C. The ins and outs of cytochrome P450s. *Biochim. Biophys. Acta, Gen. Subj.* **2007**, *1770*, 390−401.

(24) Rydzewski, J.; Nowak, W. Machine Learning Based Dimensionality Reduction Facilitates Ligand Diffusion Paths Assessment: A Case of Cytochrome P450cam. *J. Chem. Theory Comput.* **2016**, *12*, 2110−2120.

(25) Rydzewski, J.; Nowak, W. Thermodynamics of camphor migration in cytochrome P450cam by atomistic simulations. *Sci. Rep.* **2017**, *7*, 7736.

(26) Markwick, P. R.; Pierce, L. C.; Goodin, D. B.; McCammon, J. A. Adaptive Accelerated Molecular Dynamics (Ad-AMD) Revealing the Molecular Plasticity of P450cam. *J. Phys. Chem. Lett.* **2011**, *2*, 158−164.

(27) Hollingsworth, S. A.; Poulos, T. L. Molecular dynamics of the P450cam-Pdx complex reveals complex stability and novel interface contacts. *Protein Sci.* **2015**, *24*, 49−57.

(28) Batabyal, D.; Richards, L. S.; Poulos, T. L. Effect of Redox Partner Binding on Cytochrome P450 Conformational Dynamics. *J. Am. Chem. Soc.* **2017**, *139*, 13193−13199.

(29) Salomon-Ferrer, R.; Gotz, A. W.; Poole, D.; Le Grand, S.; Walker, R. C. Routine Microsecond Molecular Dynamics Simulations with AMBER on GPUs. 2. Explicit Solvent Particle Mesh Ewald. *J. Chem. Theory Comput.* **2013**, *9*, 3878−3888.

(30) Hopkins, C. W.; Le Grand, S.; Walker, R. C.; Roitberg, A. E. Long-Time-Step Molecular Dynamics through Hydrogen Mass Repartitioning. *J. Chem. Theory Comput.* **2015**, *11*, 1864−1874.

(31) Roe, D. R.; Cheatham, T. E., 3rd PTRAJ and CPPTRAJ: Software for Processing and Analysis of Molecular Dynamics Trajectory Data. *J. Chem. Theory Comput.* **2013**, *9*, 3084−3095.

(32) Humphrey, W.; Dalke, A.; Schulten, K. VMD: visual molecular dynamics. *J. Mol. Graphics* **1996**, *14*, 33−38.

(33) Asciutto, E. K.; Pochapsky, T. C. Some Surprising Implications of NMR-directed Simulations of Substrate Recognition and Binding by Cytochrome P450cam (CYP101A1). *J. Mol. Biol.* **2018**, *430*, 1295−1310.

(34) Asciutto, E. K.; Young, M. J.; Madura, J.; Pochapsky, S. S.; Pochapsky, T. C. Solution structural ensembles of substrate-free cytochrome P450(cam). *Biochemistry* **2012**, *51*, 3383−3393.

DOI: 10.1021/jacs.8b09441
J. Am. Chem. Soc. 2018, 140, 16222−16228

(35) Marden, M. C.; Hui Bon Hoa, G. P-450 binding to substrates camphor and linalool versus pressure. *Arch. Biochem. Biophys.* **1987**, *253*, 100−107.
(36) Lipscomb, J. D. Electron paramagnetic resonance detectable states of cytochrome P-450cam. *Biochemistry* **1980**, *19*, 3590−3599.
(37) Lange, R.; Bonfils, C.; Debey, P. The low-spin/high-spin transition equilibrium of camphor-bound cytochrome P-450. Effects of medium and temperature on equilibrium data. *Eur. J. Biochem.* **1977**, *79*, 623−628.
(38) Narasimhulu, S.; Havran, L. M.; Axelsen, P. H.; Winkler, J. D. Interactions of substrate and product with cytochrome P450: P4502B4 versus P450cam. *Arch. Biochem. Biophys.* **1998**, *353*, 228−238.
(39) Yao, H.; McCullough, C. R.; Costache, A. D.; Pullela, P. K.; Sem, D. S. Structural evidence for a functionally relevant second camphor binding site in P450cam: model for substrate entry into a P450 active site. *Proteins: Struct., Funct., Genet.* **2007**, *69*, 125−138.
(40) Wand, A. J. Dynamic activation of protein function: a view emerging from NMR spectroscopy. *Nat. Struct. Biol.* **2001**, *8*, 926−931.
(41) Wand, A. J. On the dynamic origins of allosteric activation. *Science* **2001**, *293*, 1395.
(42) Nagano, S.; Tosha, T.; Ishimori, K.; Morishima, I.; Poulos, T. L. Crystal structure of the cytochrome p450cam mutant that exhibits the same spectral perturbations induced by putidaredoxin binding. *J. Biol. Chem.* **2004**, *279*, 42844−42849.
(43) Tosha, T.; Yoshioka, S.; Ishimori, K.; Morishima, I. L358P mutation on cytochrome P450cam simulates structural changes upon putidaredoxin binding: the structural changes trigger electron transfer to oxy-P450cam from electron donors. *J. Biol. Chem.* **2004**, *279*, 42836−42843.
(44) Yoshioka, S.; Tosha, T.; Takahashi, S.; Ishimori, K.; Hori, H.; Morishima, I. Roles of the proximal hydrogen bonding network in cytochrome P450cam-catalyzed oxygenation. *J. Am. Chem. Soc.* **2002**, *124*, 14571−14579.
(45) Koga, H.; Yamaguchi, E.; Matsunaga, K.; Aramaki, H.; Horiuchi, T. Cloning and nucleotide sequences of NADH-putidaredoxin reductase gene (camA) and putidaredoxin gene (camB) involved in cytochrome P-450cam hydroxylase of Pseudomonas putida. *J. Biochem.* **1989**, *106*, 831−836.
(46) Aramaki, H.; Kabata, H.; Takeda, S.; Itou, H.; Nakayama, H.; Shimamoto, N. Formation of repressor-inducer-operator ternary complex: negative cooperativity of d-camphor binding to CamR. *Genes Cells* **2011**, *16*, 1200−1207.

DOI: 10.1021/jacs.8b09441
J. Am. Chem. Soc. 2018, 140, 16222−16228